

Emergent global biogeography of marine fish food webs


P. Daniël van Denderen^{1*}, Colleen M. Petrik², Charles A. Stock³ & Ken H. Andersen¹

¹ Centre for Ocean Life, DTU Aqua, Technical University of Denmark, Lyngby, Denmark

² Department of Oceanography, Texas A&M University, MS 3146, College Station, TX 77845

³ NOAA, Geophysical Fluid Dynamics Laboratory, Princeton, NJ 08540

* **Corresponding author:** P. Daniël van Denderen. Address: DTU Aqua, Kemitorvet, Bygning 202, 2800 Kgs. Lyngby Denmark. Email: pdvd@aqu.dtu.dk

Acknowledgements: We thank FD González Taboada for his comments on the manuscript. PDvD and KHA were funded by the Centre for Ocean Life, a VKR center of excellence supported by the Villum Foundation. KHA was further funded by the *European Union's Horizon 2020 research and innovation programme* under grant agreement No 817806 .

Data availability statement: Data and code for all analyses are available on github via Zenodo DOI: [10.5281/zenodo.3923824](https://doi.org/10.5281/zenodo.3923824)

Biosketch: The authors are developing mechanistic trait-based approaches to study life in the ocean. These approaches are used for large-scale assessments of climate change, fisheries and marine ecosystem functions.

This is the author manuscript accepted for publication and has undergone full peer review but has not been through the copyediting, typesetting, pagination and proofreading process, which may lead to differences between this version and the [Version of Record](#). Please cite this article as [doi: 10.1111/GEB.13348](https://doi.org/10.1111/GEB.13348)

This article is protected by copyright. All rights reserved

1

2 DR. DANIËL VAN DENDEREN (Orcid ID : 0000-0001-6351-0241)

3 DR. COLLEEN PETRIK (Orcid ID : 0000-0003-3253-0455)

4

5

6 Article type : Research Article

7

8

9 **Emergent global biogeography of marine fish food webs**

10 **Running title:** Biogeography of fish food webs

11

12 **Abstract**

13 **Aim:** Understanding how fish food webs emerge from planktonic and benthic production that
14 sustain them is an important challenge for predicting fisheries production under climate change
15 and quantifying the role of fish in carbon and nutrient cycling. We examine if a trait-based fish
16 community model using the fish traits of maximum body weight and vertical habitat strategy can
17 meet this challenge by globally representing fish food web diversity.

18 **Location:** Global oceans

19 **Time period:** Predictions are representative of the early 1990s

20 **Major taxa studied:** Marine teleost fish

21 **Method:** We present a size- and trait-based fish community model that explicitly resolves the
22 dependence of fish on pelagic and benthic energy pathways to globally predict fish food web
23 biogeography. The emergent food web structures are compared with regionally-calibrated
24 models in three different ecosystem types and used to estimate two fish ecosystem functions:
25 potential fisheries production and benthic-pelagic coupling.

26 **Results:** Variations in pelagic-benthic energy pathways and seafloor depth drive the emergent
27 biogeography of fish food webs from shelf systems to the open ocean, and across the global
28 ocean. Most shelf regions have high benthic production, which favors demersal fish that feed on
29 pelagic and benthic pathways. Continental slopes also show a coupling of benthic and pelagic
30 pathways, sustained through vertically migrating and interacting mesopelagic and deep-sea
31 demersal fish. Open ocean fish communities are primarily structured around the pelagic pathway.
32 Global model results compare favorably with data-driven regional food web models, suggesting
33 that maximum weight and vertical behavior can capture large-scale variations in food web
34 structure.

35 **Main conclusion:** Mechanistically linking ocean productivity with upper trophic levels using a
36 size- and trait-based fish community model results in spatial variations in food web structure.
37 Energy pathways vary with ocean productivity and seabed depth, thereby shaping the dominant
38 traits and fish communities across ocean biomes.

39
40 **Keywords:**

41 Benthic-pelagic coupling, Energy chains, Fish, Mesopelagic, Size-based models, Trait-based
42 ecology

43 **Introduction**

44 Fish are a globally important food source and are a key component of biodiversity and ecosystem
45 functions in marine systems worldwide (FAO, 2016; Villéger et al., 2017). With shifting climatic
46 conditions, there is a growing need to understand current links between ocean productivity and
47 fish food web variations in order to predict future changes. These predictions are needed to
48 assess future changes in fisheries production (Lotze et al., 2019; Stock et al., 2017), as well as to
49 address how the ecological role of fish in marine systems may change and impact nutrient
50 cycling and carbon sequestration (Saba et al., 2021; Wilson et al., 2009).

51 Recent advances in size-based ecology have resulted in models that are well-suited to estimate
52 energy transfer from plankton to the upper trophic levels, i.e. piscivorous fish, of marine pelagic
53 food webs. The size-based models derive fish communities as a size distribution and represent
54 differences among species only by the trait maximum body weight (Andersen, Jacobsen, et al.,
55 2015; Pope et al., 2006). The models link all physiological processes and patterns of predation

56 and mortality, i.e. big fish eat small fish, to individual body weight, which is a simplification that
57 enables characterizing fish communities with few parameters. As a result, size-based models
58 have been used across marine regions to describe fish communities and implemented in a global
59 context, e.g. Jacobsen et al. (2017) and Jennings & Collingridge (2015).

60 Empirical work on body size and food web structure has suggested that predictions of feeding
61 interactions can be considerably improved when body size is not used in isolation but in
62 interaction with other traits (Eklöf et al., 2013). For fish communities, there is a growing
63 recognition of the importance of a vertical-trait axis to incorporate the vertical structure of a fish
64 community, i.e. how biomass and feeding interactions are distributed across the water column
65 (Giraldo et al., 2017; Pecuchet et al., 2020). This vertical structure of a fish community is partly
66 driven by variations in diet, e.g. some fish are associated with the bottom habitat, where they
67 feed on benthic invertebrates, whereas other fish have a more planktivorous diet and live in the
68 water-column. The vertical structure is also organized by the availability of light and oxygen
69 (Bianchi, Stock, et al., 2013). Millions of fish migrate to the deeper ocean during the day to
70 escape predatory fish in the well-lit surface waters thereby actively transporting carbon to depth
71 through respiration and other processes, such as excretion and death (Irigoiien et al., 2014). The
72 vertical structure of a fish community hence influences the biogeochemical fluxes of oxygen and
73 carbon in the water column (Bianchi, Galbraith, et al., 2013; Saba et al., 2021). The vertical
74 structure may further drive fish food web variations associated with important ecosystem
75 functions such as benthic-pelagic coupling and potential fisheries production (Petrik et al., 2019;
76 van Denderen et al., 2018). Consequently, there have been rapid developments in regional and
77 global modelling systems to predict the vertical structure of marine fish communities (Anderson
78 et al., 2018; Aumont et al., 2018; Blanchard et al., 2012; Lehodey et al., 2010; Maury, 2010).
79 Yet, none of these studies has so far considered vertically distinct pelagic habitats together with
80 the important role of the benthic seabed ecosystem as food for fish.

81 To represent fish in the benthic habitat and vertically distinct pelagic habitats, we introduce a
82 vertical trait axis into a size- and trait-based modelling framework (FEISTY) previously used to
83 simulate (epi)pelagic and demersal fish (Petrik et al., 2019). We implement the model for five
84 fish guilds that differ in their maximum body weight and vertical habitat strategy (Fig. 1). We
85 assert that this functional diversity ensures a generic representation of fish diversity to resolve

86 global fisheries catches and active carbon export to depth. The aims of this paper are: 1) to
87 predict the emergent biogeography of fish food web types based on large-scale variations in the
88 biomass of individual fish guilds and their feeding interactions with shifting environmental
89 conditions; 2) to compare the predicted fish food webs with regionally-calibrated models in three
90 different ecosystem types; and 3) to estimate two ecosystem functions, potential fisheries
91 production and benthic-pelagic coupling by demersal fish, from the emerging fish community
92 food web structures.

93 **Methods**

94 Overview of model structure

95 The fish food web is described by a size-structured biomass model that follows the framework
96 developed by de Roos et al. (2008) and was used previously by Petrik et al. (2019) to estimate
97 global fish production of forage, large pelagic and demersal fish. The model incorporates food-
98 dependent somatic growth and reproduction following a standard bioenergetic budget for size-
99 and physiologically structured models (Andersen, Jacobsen, et al., 2015; de Roos et al., 2008) (SI
100 1, Table S1.1). Differences among fish guilds are represented by the traits maximum body
101 weight and vertical habitat strategy. The trait maximum body weight represents a trade-off
102 between reproductive output and adult maximum size (Andersen & Beyer, 2006). The trait
103 vertical habitat strategy describes the vertical distribution of the different fish guilds and
104 resources along the water column. Fish vertical distribution varies within a guild by size and
105 day/night through vertical migrations and is imposed following observations from the literature
106 (SI 2). Fish interact through predator-prey interactions that depend on habitat overlap in the
107 water column and the rule that big predators eat smaller prey (Barnes et al., 2010).

108 We use the model to predict fish guild biomass and food web structure on a 1° spatial grid across
109 the global ocean. These predictions are driven by estimates of zooplankton and the energy supply
110 to the benthos from a high-resolution ($1/10^\circ$ spatial grid) Carbon, Ocean Biogeochemistry and
111 Lower Trophics (COBALT) ecosystem model from a climatology of GFDL's Earth System
112 Model (ESM2.6) representative of the early 1990s (hereafter termed ESM2.6-COBALT) (Stock
113 et al., 2014, 2017), water column temperatures and seafloor and euphotic depth (see SI 3 for data
114 sources). We further examine the changes in fish guild biomass and food web structure as a

115 function of seafloor depth for different idealized resource productivity and water column
116 temperature scenarios (see SI 4 for data sources).

117 Fish guilds

118 We implement the model for five fish guilds (Fig. 1). We build upon the guild classification of
119 Petrik et al., (2019) comprising three guilds with fish primarily important for global fisheries
120 catches: 1) epipelagic fish, such as sardines and anchovies commonly referred to as forage fish,
121 with a small maximum weight that feed in the upper water column on zooplankton, 2) large
122 pelagic predators, such as billfish and tunas, that feed on plankton in earlier life stages and prey
123 upon fish later in life, and 3) large demersal fish, such as cod, haddock and halibut, that feed as
124 larvae in the water column and on benthic invertebrates and pelagic fish later in life. These three
125 guilds largely ignore the mid-water habitats in open ocean environments.

126 Two other guilds are common in open ocean mid-water habitats where they contribute to carbon
127 export to depth: 4) mesopelagic fish and 5) mid-water predators. Mesopelagic fish, such as
128 lanternfishes and bristlemouths, are most dominant in the open ocean (Irigoiien et al., 2014).
129 These fish have a small maximum weight and are adapted to living in a twilight environment
130 (Fig. 1). Mesopelagic fish are known for their diel vertical migration behavior, being at depth
131 during the day and at the surface during night. The migrations of the mesopelagic fish
132 community attract large pelagic predators to the twilight zone for daytime feeding (Evans et al.,
133 2008). Predation on the mesopelagic fish community also occurs by demersal fish, e.g.
134 slickheads and rattails, that feed on the migrating mesopelagic community during day and
135 migrate to deeper waters during night to feed at the seafloor (Trueman et al., 2014). Lastly, the
136 mid-water predators occupying the twilight zone, e.g. sabertooths and barracudinas, are a third
137 predator group that preys on the mesopelagic fish community (Drazen & Sutton, 2017; Hopkins
138 et al., 1996).

139 We assume that epipelagic fish, large pelagics and demersal fish make up the fish community in
140 shelf regions, i.e. regions < 250 meters in depth. On continental slopes (250-2000 meters) and
141 open ocean regions, all fish guilds may coexist. The vertical distribution of the different fish
142 guilds is shown in Fig. 2 and further explained in SI 2.

143 We parameterize epipelagic/forage and mesopelagic fish with a maximum body weight of 250 g
144 (lower limit of weight at maturation is 0.5 g) and the three larger guilds with a maximum body
145 weight of 125 kg (lower limit of weight at maturation is 250 g). For computational efficiency, we
146 represent the size-distribution of epipelagic and mesopelagic fish in four size-classes and the
147 three larger guilds in six classes. The model outcome is largely insensitive to the exact number of
148 size-classes used (SI 5).

149 All fish parameters beside maximum body weight and vertical habitat strategy are similar across
150 guilds and based on general fish physiology and mass-scaling principles (SI 1, Table S1.2). The
151 physiological rates (clearance, metabolic and maximum consumption rates) scale with
152 temperature. This scaling corresponds to a Q_{10} of 1.88, where Q_{10} shows the rate of change of the
153 parameters as a result of an increase of 10°C . This value, which originates with phytoplankton
154 growth studies (Eppley, 1972) and is within the range of values reported for zooplankton growth
155 and ingestion (Hansen, 1997), was used to scale all biological processes in the underlying
156 plankton food web model (Stock et al., 2014) and is carried through to the fish model
157 configuration. Since ambient temperatures vary in the water column, an average temperature per
158 guild and size class is estimated by integrating water column temperatures over the vertical
159 distribution of each fish guild and size class. More details on the model's equations, assumptions
160 and parameters can be found in SI 2.

161 Zooplankton and benthic resources

162 We include two zooplankton resources and one benthic resource following Petrik et al. (2019).
163 The smaller zooplankton group represents small to medium-sized copepods in the size range
164 $2 \cdot 10^{-6} - 0.001$ g (0.2 – 2 mm) and the larger group represents large copepods and krill in the size
165 range $0.001 - 0.5$ g (2 – 20 mm). In shelf regions, the zooplankton groups are assumed to be
166 distributed in the upper water column with a maximum concentration at the surface of the water
167 column, whereas part of the zooplankton in each size group is assumed to make diel vertical
168 migrations in slope and open oceans regions (see further SI 2). Benthos consist of one size group
169 that represents benthic fauna from small annelids of $5 \cdot 10^{-4}$ g to larger organisms of 125 g, such
170 as echinoderms and bivalves, and are concentrated at the seafloor.

171 All resource groups follow semi-chemostat dynamics, with a turnover rate and a maximum
172 biomass density (SI 1, table S1.1 and SI 2). The maximum resource production, described as the

173 product of these two terms, is scaled to the medium and large zooplankton productivities on a 1°
174 grid from ESM2.6-COBALT (Stock et al., 2014, 2017). Such a scaling of zooplankton
175 productivities is both done for the global predictions as well as the theoretical scenarios, as
176 explained in SI 3 and SI 4 respectively. Benthic maximum production is modeled in two
177 different ways. In the global predictions, benthic maximum production is estimated from
178 ESM2.6-COBALT output of the detritus flux reaching the seabed (SI 3). In the theoretical
179 scenarios, benthic maximum production depends on both the detrital export flux out of the
180 euphotic zone and seafloor depth. For the latter, benthic maximum production declines for
181 seafloor depths that are deeper than the euphotic depth with a power law function that represents
182 remineralization of detritus in the water column (Martin et al., 1987; Suess, 1980) (SI 1, table
183 S1.1).

184 The ESM2.6-COBALT outputs drive fish guild biomass and food web predictions. The ESM2.6-
185 COBALT model, which is described and evaluated in Stock et al. (2017), has an ocean resolution
186 of 1/10°. The output is averaged to a 1° grid for use in this application. The 1° patterns still
187 reflect the integrated effect of fine scale processes, which is especially important to represent
188 coastal areas. There are two main shortcomings with the ESM2.6-COBALT predictions that are
189 likely to influence our outcomes: 1) it underpredicts very high chlorophyll in near-shore regions,
190 and 2) it is limited in representing the complex dynamics in inland seas. Nevertheless, both
191 across ocean biomes as well as across globally-distributed large marine ecosystems, ESM2.6-
192 COBALT robustly captures the primary differences in chlorophyll, primary production, export
193 fluxes, and medium and large zooplankton biomass (Stock et al., 2017). We may therefore
194 expect that despite the potential for regional bias, ESM2.6-COBALT encapsulates the primary
195 contrasts in zooplankton and benthic productivity across the disparate ecosystem types
196 considered in our analysis.

197 Analysis

198 At each grid cell, we run the fish model for 300 years and take the average of the last 60 years
199 (by which time the model has converged to an equilibrium or stable attractor). Initial conditions
200 of fish biomass are 0.01 g wet weight m⁻² for each size class and resource biomass is 10% of
201 maximum biomass density.

202 We classify the observed food webs into different types, based on the relative biomasses of the
203 five fish guilds, to map the emergent biogeography of the fish food webs (objective 1). We
204 afterwards compare guild biomasses and the fluxes between them from our modelling output
205 with three regionally-calibrated Ecopath with Ecosim (EwE) models, downloaded from EcoBase
206 (Colléter et al., 2013) (objective 2). We use EwE models for validation as they offer a data-
207 driven inversion for the food web characteristics (Christensen & Walters, 2004; Polovina, 1984)
208 to assess against feeding fluxes between fish guilds and biomass of fish guilds arising in our
209 model. The three EwE models reflect different ecosystem types, 1) the North Sea shelf with a
210 relatively strong benthic pathway (Mackinson & Daskalov, 2008), 2) the Peruvian shelf with a
211 relatively strong pelagic pathway (Jarre-Teichmann & Pauly, 1993) and 3) a continental slope
212 region off the coast of Scotland (Howell et al., 2009). This comparison requires the classification
213 of the EwE fish species into one of the five fish guilds used in our model (see SI 6).

214 Lastly, we estimate two ecosystem functions, potential fisheries production and benthic-pelagic
215 coupling by demersal fish (objective 3). Potential fisheries production is estimated as a fraction
216 of the energy flowing from juveniles to the fished adults. Classic surplus production fisheries
217 models show that the maximum sustainable yield to be taken from fisheries is about half of the
218 potential flux. We calculate this energy flux for epipelagic and mesopelagic guilds (maximum
219 size is 250 g) based on the energy flowing from size-class 2 to 3 and for the other guilds
220 (maximum size >250 g) based on the energy flowing from size-class 4 to 5. For the epipelagic
221 and mesopelagic guilds, we first consider only a quarter of the total flux from size-class 2 to 3 to
222 leave additional production as food for the larger fish guilds. Benthic-pelagic coupling by
223 demersal fish shows the relative flux of energy from pelagic and benthic sources consumed by
224 demersal fish. The pelagic flux is here defined as all energy from pelagic zooplankton and the
225 four pelagic fish guilds to demersal fish, whereas the benthic flux represents demersal fish
226 feeding on benthic invertebrates and excludes cannibalism by demersal fish.

227 To disentangle the many processes from the global model output that affect fish guild biomass
228 and food web structure, we end with a theoretical analysis of the model. In this analysis, we
229 show the changes in fish guild biomass as a function of seafloor depth for different resource
230 productivity scenarios and water column temperatures. Variations in these three axes allow us to

231 mimic the primary contrasts across the range of ecosystems in the full global model, elucidating
232 drivers of cross-ecosystem contrasts.

233 **Results**

234 Emergent biogeography of fish food web types

235 Food web structure, defined by the relative biomasses of the five fish guilds at each 1° grid cell
236 (SI 1, Fig. S1.1), are predicted globally (Fig. 3). Continental shelf regions typically have a high
237 detrital flux reaching the seabed, supporting high benthic production. In these regions, demersal
238 fish are abundant as they can easily feed on both pelagic and benthic energy pathways (Fig. 3a
239 and dark orange in 3f). Demersal fish usually coexist with epipelagic fish and large pelagics.
240 There are a few shallow regions in the high arctic with low pelagic and benthic production where
241 epipelagic fish are the sole group present (not visible in Fig. 3f). Feeding on pelagic and benthic
242 energy pathways also occurs by demersal fish on continental slopes that still have a relatively
243 high flux of detritus reaching the seafloor (Fig. 3b, light orange in 3f). In these regions, adult
244 demersal fish make upward migrations during the day to feed on mesopelagic fish in the twilight
245 zone, which are further preyed upon by large pelagics. On both shelves and slopes, pelagic and
246 benthic energy pathways are therefore typically coupled through cross-habitat feeding (Fig. 3a-
247 b).

248 In the deeper open ocean regions, pelagic and benthic energy pathways are decoupled. In regions
249 with high zooplankton production, large pelagics coexist with epipelagic fish, mesopelagic fish
250 and mid-water predators (Fig. 3c, dark blue in 3f). Large parts of the open ocean are meso- and
251 oligotrophic areas with low nutrient mixing and consequently minimal new primary production
252 and low zooplankton production. The fish community in these areas is devoid of large predators
253 and gradually shifts from a community with epipelagic fish and mesopelagic fish (Fig. 3d, blue
254 in 3f), to mesopelagic fish only (Fig. 3e, light blue in 3f), to no fish in the least productive areas
255 (Fig. 3, white in 3f). The absence of fish in these limited areas indicates that fish present in
256 nature in these regions are either migratory or adapted to survive with low food in ways that are
257 not accounted for in our 5-guild model. Demersal fish are also absent in large parts of the deep
258 sea, indicating similar types of adaptations to low food and/or pulsed food events.

259 Model comparison with regional models

260 Despite the simplicity of our model, the predicted biomasses and energy flows capture the
261 general features of the regional EwE food webs well (Fig. 4). As expected, shelf regions,
262 exemplified by the North Sea and Peruvian shelves, have higher benthic biomass and strong
263 feeding fluxes towards demersal fish in both models. Both models also predict that the Peruvian
264 shelf has a stronger pelagic pathway and higher biomass of pelagic fish relative to the North Sea
265 shelf. Finally, the slope region West of Scotland has a dominant mid-water fish community in
266 both models. A closer inspection shows that the regional model of the North Sea estimates more
267 benthic biomass and higher fluxes from benthos to fish as compared with our prediction, whereas
268 the regional model West of Peru estimates higher pelagic fish biomass and feeding flux within
269 the pelagic fish community. The regional EwE model of the West Scotland slope predicts
270 stronger feeding fluxes and no epipelagic and/or large pelagic fish. Whether the absence of these
271 fish guilds in this region is a fisheries/sampling effect, the result of specific environmental
272 conditions or a misclassification of fish species into a specific guild for comparison with our
273 study (see SI 6) is difficult to determine. Regardless, the discrepancies between our simulations
274 and the EwE solution within a given system are small relative to the consistency of the cross-
275 ecosystem contrasts of primary interest herein.

276 Fish ecosystem functions

277 Fish ecosystem functions can be obtained from the food web structures determined by the model.
278 As examples, we show measures of potential fisheries production (Fig. 5a) and benthic-pelagic
279 coupling by demersal fish (Fig. 5b). The estimated fisheries production is 101 million tonnes per
280 year. As expected, potential fisheries production per area is highest in shelf seas and upwelling
281 systems that have high secondary production (Fig. 5a). Shelf and slope regions with seafloor
282 depths less than 2000 m contribute 30% of the potential production. Mesopelagic fish have a
283 potential fisheries production of 30 million tonnes per year. The potential production can be
284 increased by taking a higher flux from the small guilds (e.g. half instead of a quarter), which in
285 nature will cause a reduction in the biomass and catch of large fish due to a decline in prey fish.
286 This fishing patterns increases the potential global production to 168 million tonnes per year.

287 Benthic-pelagic coupling by demersal fish shows the relative flux of energy from pelagic and
288 benthic sources consumed by demersal fish (Fig. 5b). In most shelf and slope regions, a large
289 fraction of energy consumed by all size-classes of demersal fish is of pelagic origin. For the

290 continental slope regions, this large fraction highlights that carbon is continuously transported to
291 the deeper waters through cross-habitat feeding. There is a small fraction of pelagic energy
292 consumed by demersal fish in decoupled open ocean systems, since the early life stages are
293 feeding on zooplankton in the surface waters.

294 Theoretical analysis of fish guild biomass as a function of seafloor depth

295 The changes in fish food web structure (Fig. 3) from shelf to open ocean environments are driven
296 by changes in production of zooplankton and benthos, detrital flux and seafloor depth (Fig. 6). In
297 regions with a high pelagic production and a high detrital export flux out of the sunlit euphotic
298 zone, demersals are dominant in shallow shelf regions together with epipelagic fish (Fig. 6a-b).
299 The demersals decline in biomass with depth and this promotes large pelagics. At continental
300 slopes, mesopelagic fish become abundant and epipelagic fish decline. This shift happens due to
301 the diel vertical migrations of the zooplankton community that benefit mesopelagic fish (SI 1,
302 Fig. S1.2). Mesopelagic fish are preyed upon by large pelagics and adult deep-living demersal
303 fish on slopes. Deep-living demersals gradually decrease in biomass with depth and this decline
304 promotes mid-water predators (Fig. 6a-b). Around 2000 meters, demersals are unable to migrate
305 the large distance between the mid-water fish community and the bottom, resulting in a
306 decoupling of the energy pathways. Low pelagic production and low detrital export flux out of
307 the euphotic zone, i.e. oligotrophic regions, select for epipelagic and mesopelagic fish (Fig. 6c).
308 The productivity and abundance of these small fish is too low to support larger pelagic predators.
309 Demersal fish do survive in these conditions if there is sufficient benthic prey.

310 Changes in fish guild biomass are also affected by water column temperatures that change fish
311 physiological rates. The temperature dependencies in our model are similar for all fish guilds and
312 physiological rates and therefore have little influence on the relative dominance of fish guilds (SI
313 1, Fig. S1.3 - S1.5). As a result, higher water column temperatures mainly decrease the biomass
314 of each fish guild, and hence total fish community biomass, due to increased maintenance costs
315 (SI 1, Fig. S1.3).

316 **Discussion**

317 We modified a generic size- and trait-based fish community model (FEISTY) to predict the
318 emergent biogeography of fish food web types based on large-scale variations in fish guild
319 biomass and vertical feeding interactions with shifting environmental conditions. The result was

320 several structurally different food web types that predictably vary with seafloor depth and ocean
321 productivity. Below we expand upon the results of each of our objectives. This is followed by a
322 discussion on model limitations and a conclusion.

323 Fish food web biogeography

324 The transfer of energy from primary producers to upper trophic levels varies across marine
325 regions throughout the ocean (Ryther, 1969). Broadly speaking, the transfer of energy varies
326 cross-regionally due to differences in 1) food chain lengths that connect phytoplankton to fish,
327 and 2) the strength of pelagic and benthic energy pathways (Friedland et al., 2012; Stock et al.,
328 2017). Such processes not only affect overall fish community biomass and potential fisheries
329 catches, but also the guild distribution of fish in a community (Cresson et al., 2020; Petrik et al.,
330 2019; van Denderen et al., 2018). Our results show that the distribution of biomass between fish
331 guilds directly depends on pelagic and benthic secondary production and is strongly mediated by
332 seabed depth, which (indirectly) controls the amount of detritus reaching the seabed, fish vertical
333 behavior and fish cross-habitat feeding. The importance of these individual processes for fish
334 food web structure has been recognized for a long time. We show how these well-known bottom-
335 up structuring forces can be used to simulate fish guild biomass and feeding interactions across
336 ocean biomes on a global scale. Our study thereby mechanistically links variation in ocean
337 productivity with the upper trophic levels of marine ecosystems.

338 We used a generic trait-based configuration to estimate the structural differences in energy flow
339 in fish communities across regions. The advantage of a trait-based approach is that it does not
340 require the quantification of feeding interactions from species-based parameterizations, thereby
341 allowing characterizing fish communities with few parameters. Another advantage of a trait-
342 based approach is that its basis in physiological and ecological principles may be more robust in
343 predicting the long-term effects of climate change on fish guild biomass and associated
344 ecosystem functions than empirical relationships, e.g. Cheung et al (2016). For example, the
345 modeled fish guilds automatically adjust feeding interactions and physiological rates to new
346 environmental conditions, essentially reflecting a state where community re-assembly and
347 temperature adaptations have progressed (Kiørboe et al., 2018). Nonetheless, our predicted food
348 webs represent highly simplified fish communities that do not represent the myriad of species

349 that exist in natural systems. They are therefore primarily useful for large-scale assessments of
350 climate change, guild-based fisheries and fish ecosystem functions.

351 Model validation

352 It is difficult to determine the extent to which the model reflects empirical patterns in nature.
353 Estimates of fish biomass are available from scientific surveys for different regions, with
354 uncertainty due to variation in gear catchability, acoustic backscatter methodology and historic
355 fishing exploitation, whereas estimates of feeding fluxes are more difficult to obtain. Our initial
356 efforts at model validation were therefore to compare against regional ecosystem models whose
357 food webs have been calibrated for particular regions using data-driven inversion techniques, i.e.
358 Ecopath balances (Christensen & Walters, 2004). We found a reasonable match between our
359 modeled fish guild biomasses and feeding fluxes, and three EwE models that reflect different
360 ecosystem types. Yet, note that any difference (or similarity) could be due to the different
361 modelling frameworks.

362 At global scales, an alternative option to validate the model predictions is to compare modeled
363 fisheries catches with empirical catch reconstructions. This comparison has been done by Petrik
364 et al. (2019), using a model formulation upon which our model structure is based. This study
365 found a reasonable agreement between modeled and empirical catches of large pelagics and
366 demersal fish across large marine ecosystems. Such a comparison with empirical catch data is
367 primarily useful for heavily-fished continental shelf and upwelling regions where most of the
368 fisheries production occurs and catch provides a more reliable estimate of the relative fish
369 productivity between regions.

370 Other comparisons of our findings to observations, statistical models, and mechanistic models
371 agree on the large-scale food web structures, yet reveal nuanced differences. A more qualitative
372 comparison with empirical work in continental slope regions suggests that our model predicts
373 larger declines in demersal fish biomass with depth than is typically observed (Kallianiotis et al.,
374 2000; Mindel et al., 2016; Trueman et al., 2014). This may be due to ontogenetic migrations by
375 adult demersal fish to deeper and more offshore waters (Macpherson & Duarte, 1991), as well as
376 a larger capacity to exploit the migrating mesopelagic resource than was modeled. Nevertheless,
377 demersal fish biomass eventually declines with depth following the decline in the detrital flux
378 that reaches the seafloor (Wei et al., 2011). For open ocean pelagic systems, mesopelagic fish

379 biomass has been found to strongly correlate with ocean productivity (Irigoien et al., 2014) and
380 such effects are also found in the model. One aspect that is clearly misrepresented in the model is
381 the simulated high abundance of large pelagics in cold-water regions, where they are able to exist
382 in our model due to a high zooplankton productivity. Pelagic predators are indeed present in
383 these waters, although not as (teleost) fish but as pelagic-feeding endotherms, e.g., penguins and
384 pinnipeds, that can maintain a high body temperature and activity and outcompete large pelagic
385 fish (Grady et al., 2019).

386

387 Fish ecosystem functions

388 We estimated a potential fisheries production of 101 million tonnes per year in the model,
389 ignoring fisheries production of invertebrates. This estimate compares well with the global
390 industrial fisheries output over the last decades of approximately 100 million tonnes per year (up
391 to 130 million tonnes per year when the non-industrial fisheries are included), of which 15 to
392 20% is invertebrate fisheries (Pauly & Zeller 2016; Watson & Tidd, 2018). From our estimated
393 total, mesopelagic fish have a potential fisheries production of 30 million tonnes per year.
394 Mesopelagic fish are currently largely unfished but are seen as a major potential new food
395 resource for future global food security and nutrition through the production of fish-meal (St.
396 John et al., 2016). We found that the global potential fisheries production can be increased to 168
397 million tonnes per year when taking a higher flux from the small fish guilds, which in nature will
398 cause a reduction in the biomass and catch of large fish due to a decline in prey fish. The
399 prediction of increased catch when larger fish are at reduced biomass levels matches other
400 studies showing theoretically (Andersen, Brander, et al., 2015) and empirically in the South-East
401 China Sea (Szuwalski et al., 2017) that a fishery narrowly targeting small fish at the expense of
402 large fish can double the fisheries production. Despite the high yield, this shift in fishing strategy
403 will have a high environmental impact on biodiversity and the size-structure of marine
404 communities (Andersen & Gislason, 2017).

405 We quantified the amount of benthic-pelagic coupling by demersal fish across habitats. We
406 found that a large fraction of the demersal fish diet is prey inhabiting the pelagic realm
407 (zooplankton and/or pelagic fish) in both shelf and slope regions. As previously suggested by
408 Trueman et al. (2014), benthic-pelagic coupling by demersal fish in slope regions is driven by
409 vertically-migrating deep-living demersal fish that feed on vertically-migrating mesopelagic fish

410 in the water column. Such vertical migrations of prey and predator at continental slopes cover a
411 small proportion of the global ocean but may ensure fast carbon transport to depths up to about
412 2000 m, highlighting the need for further work on the quantification of these fluxes.

413 A natural next step is to assess how the vertical feeding strategies and vertical migrations of the
414 different fish guilds affect active carbon export to depth. Active carbon transport by fish (and
415 zooplankton) through diel vertical migrations is suggested to contribute substantially to the total
416 export of carbon (10-20% of the passive flux of carbon) below the euphotic zone (Aumont et al.,
417 2018; Bianchi, Stock, et al., 2013; Davison et al., 2013; Saba et al., 2021). For this study
418 however, we did not quantify active carbon export by fish as an ecosystem function, because the
419 depth of vertically migrating species was prescribed in the model. For the sake of predicting fish
420 food web structures, the specific depth of vertical migration is of limited importance as the
421 zooplankton and fish migrations are coupled to each other. Yet, vertical migration depth is
422 important to quantify active carbon fluxes and sequestration. One way to improve the model is to
423 use a global empirical relationship between depth of vertical migration and oxygen, temperature,
424 surface chlorophyll and the mixed layer depth (Bianchi, Stock, et al., 2013). Alternatively, the
425 depth of vertical migration of prey and predators may be obtained through explicit applications
426 of game theory (Pinti & Visser, 2018).

427 Limitations

428 The trait-based configuration used in our study diversified possible fish guilds, food web
429 structures and energy flows compared to the more commonly used size-based models. Yet, some
430 ecological processes and behaviors still had to be constrained in the model and can be further
431 refined. The primary shortcomings were: 1) feeding strategies were poorly resolved in shallow
432 regions (< 100 meters) by the trait “vertical habitat strategy” as most fish had vertically
433 overlapping distributions. Even though fish in shallow regions make substantial use of both
434 pelagic and benthic pathways (Duffill Telsnig et al., 2019; Giraldo et al., 2017), preference for a
435 pelagic or a benthic diet is evidenced in gut analyses and was therefore imposed in the model; 2)
436 feeding strategies excluded obligate benthivorous fish as we expected that such a strategy is of
437 limited importance for total demersal guild biomass; and 3) light availability and adaptations to
438 low or high light conditions were not explicitly incorporated in the model, which limited a
439 mechanistic implementation of some pelagic feeding strategies in open ocean environments,

440 sensu Langbehn & Varpe (2017). Our study further disregarded other upper trophic level
441 predators, such as elasmobranchs, cephalopods and mammals. The inclusion of any of these
442 predators requires further research to clarify their physiology and identify key traits and trade-
443 offs that foster coexistence.

444 Conclusion

445 Our work demonstrates how inclusion of fish vertical habitat strategy in a well-established size-
446 and trait-based framework allows for global-scale predictions of the food web structure of fish
447 communities. Using the model (which we name for recognizability FEISTY-VerticalTrait), we
448 show how ocean productivity and seabed depth shape the dominant traits and energy flows in
449 fish communities. Future developments of the model will allow 1) predicting dominance and
450 potential fisheries production of different fish guilds, 2) assessing the indirect ecosystem effects
451 of mesopelagic fisheries, which are a major potential resource for future global fisheries, 3)
452 quantifying active export of carbon to depth through fish diel vertical migrations and feeding
453 interactions and 4) examining all of the above in the context of global change. Our study thus
454 highlights the trait-based approach to modelling fish communities as a powerful tool to
455 mechanistically predict links between ocean productivity and fish production for fisheries, as
456 well as to quantify the ecological role of fish in marine systems.

457 References

- 458 Andersen, K. H., & Beyer, J. E. (2006). Asymptotic size determines species abundance in the
459 marine size spectrum. *The American Naturalist*, 168(1), 54–61.
460 <https://doi.org/10.1086/504849>
- 461 Andersen, K. H., Brander, K., & Ravn-Jensen, L. (2015). Trade-offs between objectives for
462 ecosystem management of fisheries. *Ecological Applications*, 25(5), 1390–1396.
463 <https://doi.org/10.1890/14-1209.1>
- 464 Andersen, K. H., & Gislason, H. (2017). Unplanned ecological engineering. *Proceedings of the*
465 *National Academy of Sciences*, 114(4), 634–635. <https://doi.org/10.1073/pnas.1620158114>
- 466 Andersen, K. H., Jacobsen, N. S., & Farnsworth, K. D. (2015). The theoretical foundations for
467 size spectrum models of fish communities. *Canadian Journal of Fisheries and Aquatic*

- 468 Sciences, 73(4), 575–588. <https://doi.org/10.1139/cjfas-2015-0230>
- 469 Anderson, T. R., Martin, A. P., Lampitt, R. S., Trueman, C. N., Henson, S. A., & Mayor, D. J.
470 (2018). Quantifying carbon fluxes from primary production to mesopelagic fish using a
471 simple food web model. *ICES Journal of Marine Science*, 76(3), 690–701.
472 <https://doi.org/10.1093/icesjms/fsx234>
- 473 Aumont, O., Maury, O., Lefort, S., & Bopp, L. (2018). Evaluating the potential impacts of the
474 diurnal vertical migration by marine organisms on marine biogeochemistry. *Global
475 Biogeochemical Cycles*, 32(11), 1622–1643. <https://doi.org/10.1029/2018GB005886>
- 476 Barnes, C., Maxwell, D., Reuman, D. C., & Jennings, S. (2010). Global patterns in predator-prey
477 size relationships reveal size dependency of trophic transfer efficiency. *Ecology*, 91(1),
478 222–232. <https://doi.org/10.1890/08-2061.1>
- 479 Bianchi, D., Galbraith, E. D., Carozza, D. A., Mislan, K. A. S., & Stock, C. A. (2013).
480 Intensification of open-ocean oxygen depletion by vertically migrating animals. *Nature
481 Geoscience*, 6(7), 545–548. <https://doi.org/10.1038/ngeo1837>
- 482 Bianchi, D., Stock, C., Galbraith, E. D., & Sarmiento, J. L. (2013). Diel vertical migration:
483 ecological controls and impacts on the biological pump in a one-dimensional ocean model.
484 *Global Biogeochemical Cycles*, 27(2), 478–491. <https://doi.org/10.1002/gbc.20031>
- 485 Blanchard, J. L., Jennings, S., Holmes, R., Harle, J., Merino, G., Allen, J. I., Holt, J., Dulvy, N.
486 K., & Barange, M. (2012). Potential consequences of climate change for primary production
487 and fish production in large marine ecosystems. *Phil. Trans. R. Soc. B*, 367(1605), 2979–
488 2989. <https://doi.org/10.1098/rstb.2012.0231>
- 489 Cheung, W. W. L., Frölicher, T. L., Asch, R. G., Jones, M. C., Pinsky, M. L., Reygondeau, G.,
490 Rodgers, K. B., Rykaczewski, R. R., Sarmiento, J. L., Stock, C., & Watson, J. R. (2016).
491 Building confidence in projections of the responses of living marine resources to climate
492 change. *ICES Journal of Marine Science*, 73(5), 1283–1296.
493 <https://doi.org/10.1093/icesjms/fsv250>
- 494 Christensen, V., & Walters, C. J. (2004). Ecopath with Ecosim: methods, capabilities and

- 495 limitations. *Ecological Modelling*, 172(2–4), 109–139.
496 <https://doi.org/10.1016/j.ecolmodel.2003.09.003>
- 497 Colléter, M., Valls, A., Guitton, J., Lyne, M., Arreguín-Sánchez, F., Christensen, V., Gascuel,
498 D., & Pauly, D. (2013). EcoBase: a repository solution to gather and communicate
499 information from EwE models. <https://doi.org/10.14288/1.0354309>
- 500 Cresson, P., Chauvelon, T., Bustamante, P., Bănar, D., Baudrier, J., Le Loc'h, F., Mauffret, A.,
501 Mialet, B., Spitz, J., & Wessel, N. (2020). Primary production and depth drive different
502 trophic structure and functioning of fish assemblages in French marine ecosystems.
503 *Progress in Oceanography*, 186, 102343. <https://doi.org/10.1016/j.pocean.2020.102343>
- 504 Davison, P. C., Checkley, D. M., Koslow, J. A., & Barlow, J. (2013). Carbon export mediated by
505 mesopelagic fishes in the northeast Pacific Ocean. *Progress in Oceanography*, 116, 14–30.
506 <https://doi.org/10.1016/j.pocean.2013.05.013>
- 507 de Roos, A. M., Schellekens, T., van Kooten, T., van de Wolfshaar, K. E., Claessen, D., &
508 Persson, L. (2008). Simplifying a physiologically structured population model to a stage-
509 structured biomass model. *Theoretical Population Biology*, 73(1), 47–62.
510 <https://doi.org/10.1016/j.tpb.2007.09.004>
- 511 Drazen, J. C., & Sutton, T. T. (2017). Dining in the deep: the feeding ecology of deep-sea fishes.
512 *Annual Review of Marine Science*, 9(1), 337–366. [https://doi.org/10.1146/annurev-marine-](https://doi.org/10.1146/annurev-marine-010816-060543)
513 [010816-060543](https://doi.org/10.1146/annurev-marine-010816-060543)
- 514 Duffill Telsnig, J. I., Jennings, S., Mill, A. C., Walker, N. D., Parnell, A. C., & Polunin, N. V. C.
515 (2019). Estimating contributions of pelagic and benthic pathways to consumer production in
516 coupled marine food webs. *Journal of Animal Ecology*, 88(3), 405–415.
517 <https://doi.org/10.1111/1365-2656.12929>
- 518 Eklöf, A., Jacob, U., Kopp, J., Bosch, J., Castro-Urgal, R., Chacoff, N. P., Dalsgaard, B., de
519 Sassi, C., Galetti, M., & Guimarães, P. R. (2013). The dimensionality of ecological
520 networks. *Ecology Letters*, 16(5), 577–583. <https://doi.org/10.1111/ele.12081>
- 521 Eppley, R. W. (1972). Temperature and phytoplankton growth in the sea. *Fish. Bull*, 70(4),

522 1063–1085.

523 Evans, K., Langley, A., Clear, N. P., Williams, P., Patterson, T., Sibert, J., Hampton, J., & Gunn,
524 J. S. (2008). Behaviour and habitat preferences of bigeye tuna (*Thunnus obesus*) and their
525 influence on longline fishery catches in the western Coral Sea. *Canadian Journal of*
526 *Fisheries and Aquatic Sciences*, 65(11), 2427–2443. <https://doi.org/10.1139/F08-148>

527 FAO. (2016). *The State of World Fisheries and Aquaculture 2016. Contributing to food security*
528 *and nutrition for all*. Rome. 200 pp.

529 Friedland, K. D., Stock, C., Drinkwater, K. F., Link, J. S., Leaf, R. T., Shank, B. V, Rose, J. M.,
530 Pilskaln, C. H., & Fogarty, M. J. (2012). Pathways between primary production and
531 fisheries yields of Large Marine Ecosystems. *PLoS ONE*, 7(1), e28945.
532 <https://doi.org/10.1371/journal.pone.0028945>

533 Giraldo, C., Ernande, B., Cresson, P., Kopp, D., Cachera, M., Travers-Trolet, M., & Lefebvre, S.
534 (2017). Depth gradient in the resource use of a fish community from a semi-enclosed sea.
535 *Limnology and Oceanography*, 62(5), 2213–2226. <https://doi.org/10.1002/lno.10561>

536 Grady, J. M., Maitner, B. S., Winter, A. S., Kaschner, K., Tittensor, D. P., Record, S., Smith, F.
537 A., Wilson, A. M., Dell, A. I., Zarnetske, P. L., Wearing, H. J., Alfaro, B., & Brown, J. H.
538 (2019). Metabolic asymmetry and the global diversity of marine predators. *Science*,
539 363(6425), eaat4220. <https://doi.org/10.1126/science.aat4220>

540 Hansen, B. W. (1997). Zooplankton grazing and growth: Scaling within the 2-2,000- μ m body
541 size range. *Limnol. Oceanogr*, 42, 687–704. <https://doi.org/10.4319/lo.1997.42.4.0687>

542 Hopkins, T. L., Sutton, T. T., & Lancraft, T. M. (1996). The trophic structure and predation
543 impact of a low latitude midwater fish assemblage. *Progress in Oceanography*, 38(3), 205–
544 239. [https://doi.org/10.1016/S0079-6611\(97\)00003-7](https://doi.org/10.1016/S0079-6611(97)00003-7)

545 Howell, K., Heymans, J. J., Gordon, J. D. M., Ayers, M., & Jones, E. (2009). DEEPFISH
546 Project: applying an ecosystem approach to the sustainable management of deep-water
547 fisheries. Part 1: Development of an Ecopath with Ecosim model.

548 Irigoien, X., Klevjer, T. A., Røstad, A., Martinez, U., Boyra, G., Acuña, J. L., Bode, A.,

- 549 Echevarria, F., Gonzalez-Gordillo, J. I., Hernandez-Leon, S., Agusti, S., Aksnes, D. L.,
550 Duarte, C. M., & Kaartvedt, S. (2014). Large mesopelagic fishes biomass and trophic
551 efficiency in the open ocean. *Nature Communications*, 5, 3271.
552 <https://doi.org/10.1038/ncomms4271>
- 553 Jacobsen, N. S., Burgess, M. G., & Andersen, K. H. (2017). Efficiency of fisheries is increasing
554 at the ecosystem level. *Fish and Fisheries*, 18(2), 199–211.
555 <https://doi.org/10.1111/faf.12171>
- 556 Jarre-Teichmann, A., & Pauly, D. (1993). Seasonal changes in the Peruvian upwelling
557 ecosystem. *Trophic Models of Aquatic Ecosystems*, 307–314.
- 558 Jennings, S., & Collingridge, K. (2015). Predicting consumer biomass, size-Structure,
559 production, catch potential, responses to fishing and associated uncertainties in the world's
560 marine ecosystems. *PLOS ONE*, 10(7), e0133794.
561 <https://doi.org/10.1371/journal.pone.0133794>
- 562 Kallianiotis, A., Sophronidis, K., Vidoris, P., & Tselepides, A. (2000). Demersal fish and
563 megafaunal assemblages on the Cretan continental shelf and slope (NE Mediterranean):
564 seasonal variation in species density, biomass and diversity. *Progress in Oceanography*,
565 46(2), 429–455. [https://doi.org/10.1016/S0079-6611\(00\)00028-8](https://doi.org/10.1016/S0079-6611(00)00028-8)
- 566 Kjørboe, T., Visser, A., & Andersen, K. H. (2018). A trait-based approach to ocean ecology.
567 *ICES Journal of Marine Science*, 75(6), 1849–1863. <https://doi.org/10.1093/icesjms/fsy090>
- 568 Langbehn, T. J., & Varpe, Ø. (2017). Sea-ice loss boosts visual search: fish foraging and
569 changing pelagic interactions in polar oceans. *Global Change Biology*, 23(12), 5318–5330.
570 <https://doi.org/10.1111/gcb.13797>
- 571 Lehodey, P., Murtugudde, R., & Senina, I. (2010). Bridging the gap from ocean models to
572 population dynamics of large marine predators: a model of mid-trophic functional groups.
573 *Progress in Oceanography*, 84(1), 69–84. <https://doi.org/10.1016/j.pocean.2009.09.008>
- 574 Lotze, H. K., Tittensor, D. P., Bryndum-Buchholz, A., Eddy, T. D., Cheung, W. W. L.,
575 Galbraith, E. D., Barange, M., Barrier, N., Bianchi, D., & Blanchard, J. L. (2019). Global

- 576 ensemble projections reveal trophic amplification of ocean biomass declines with climate
577 change. *Proceedings of the National Academy of Sciences*, 116(26), 12907–12912.
578 <https://doi.org/10.1073/pnas.1900194116>
- 579 Mackinson, S., & Daskalov, G. (2008). An ecosystem model of the North Sea to support an
580 ecosystem approach to fisheries management: description and parameterisation.
- 581 Macpherson, E., & Duarte, C. M. (1991). Bathymetric trends in demersal fish size: is there a
582 general relationship? *Marine Ecology Progress Series*, 103–112.
583 <https://doi.org/10.3354/meps071103>
- 584 Martin, J. H., Knauer, G. A., Karl, D. M., & Broenkow, W. W. (1987). VERTEX: carbon cycling
585 in the northeast Pacific. *Deep Sea Research Part A. Oceanographic Research Papers*,
586 34(2), 267–285. [https://doi.org/10.1016/0198-0149\(87\)90086-0](https://doi.org/10.1016/0198-0149(87)90086-0)
- 587 Maury, O. (2010). An overview of APECOSM, a spatialized mass balanced “Apex Predators
588 ECOSystem Model” to study physiologically structured tuna population dynamics in their
589 ecosystem. *Progress in Oceanography*, 84(1), 113–117.
590 <https://doi.org/10.1016/j.pocean.2009.09.013>
- 591 Mindel, B. L., Webb, T. J., Neat, F. C., & Blanchard, J. L. (2016). A trait-based metric sheds
592 new light on the nature of the body size–depth relationship in the deep sea. *Journal of*
593 *Animal Ecology*, 85(2), 427–436. <https://doi.org/10.1111/1365-2656.12471>
- 594 Pauly, D., & Zeller, D. (2016). Catch reconstructions reveal that global marine fisheries catches
595 are higher than reported and declining. *Nature Communication* 7, 10244.
596 <https://doi.org/10.1038/ncomms10244>
- 597 Pecuchet, L., Blanchet, M.-A., Frainer, A., Husson, B., Jørgensen, L. L., Kortsch, S., &
598 Primicerio, R. (2020). Novel feeding interactions amplify the impact of species
599 redistribution on an Arctic food web. *Global Change Biology*, 26, 4894–4906.
600 <https://doi.org/10.1111/gcb.15196>
- 601 Petrik, C. M., Stock, C. A., Andersen, K. H., van Denderen, P. D., & Watson, J. R. (2019).
602 Bottom-up drivers of global patterns of demersal, forage, and pelagic fishes. *Progress in*

- 603 Oceanography, 176, 102124. <https://doi.org/10.1016/j.pocean.2019.102124>
- 604 Pinti, J., & Visser, A. W. (2018). Predator-prey games in multiple habitats reveal mixed
605 strategies in diel vertical migration. *The American Naturalist*, 193(3), E65–E77.
606 <https://doi.org/10.1086/701041>
- 607 Polovina, J. J. (1984). Model of a coral reef ecosystem. *Coral Reefs*, 3(1), 1–11.
608 <https://doi.org/10.1007/BF00306135>
- 609 Pope, J. G., Rice, J. C., Daan, N., Jennings, S., & Gislason, H. (2006). Modelling an exploited
610 marine fish community with 15 parameters – results from a simple size-based model. *ICES*
611 *Journal of Marine Science*, 63(6), 1029–1044.
612 <https://doi.org/10.1016/j.icesjms.2006.04.015>
- 613 Ryther, J. H. (1969). Photosynthesis and fish production in the sea. *Science*, 166(3901), 72–76.
614 <https://doi.org/10.1126/science.166.3901.72>
- 615 Saba, G. K., Burd, A. B., Dunne, J. P., Hernández-León, S., Martin, A. H., Rose, K. A.,
616 Salisbury, J., Steinberg, D. K., Trueman, C. N., Wilson, R. W., & Wilson, S. E. (2021).
617 Toward a better understanding of fish-based contribution to ocean carbon flux. *Limnology*
618 *and Oceanography*, 66, 1639–1664. <https://doi.org/10.1002/lno.11709>
- 619 St. John, M. A., Borja, A., Chust, G., Heath, M., Grigorov, I., Mariani, P., Martin, A. P., &
620 Santos, R. S. (2016). A dark hole in our understanding of marine ecosystems and their
621 services: perspectives from the mesopelagic community. *Frontiers in Marine Science*, 3, 31.
622 <https://doi.org/10.3389/fmars.2016.00031>
- 623 Stock, C. A., Dunne, J. P., & John, J. G. (2014). Global-scale carbon and energy flows through
624 the marine planktonic food web: an analysis with a coupled physical–biological model.
625 *Progress in Oceanography*, 120, 1–28. <https://doi.org/10.1016/j.pocean.2013.07.001>
- 626 Stock, C. A., John, J. G., Rykaczewski, R. R., Asch, R. G., Cheung, W. W. L., Dunne, J. P.,
627 Friedland, K. D., Lam, V. W. Y., Sarmiento, J. L., & Watson, R. A. (2017). Reconciling
628 fisheries catch and ocean productivity. *Proceedings of the National Academy of Sciences*,
629 114(8), E1441–E1449. <https://doi.org/10.1073/pnas.1610238114>

- 630 Suess, E. (1980). Particulate organic carbon flux in the oceans-surface productivity and oxygen
631 utilization. *Nature*, 288(5788), 260–263. <https://doi.org/10.1038/288260a0>
- 632 Szuwalski, C. S., Burgess, M. G., Costello, C., & Gaines, S. D. (2017). High fishery catches
633 through trophic cascades in China. *Proceedings of the National Academy of Sciences*,
634 114(4), 717–721. <https://doi.org/10.1073/pnas.1612722114>
- 635 Trueman, C. N., Johnston, G., O’Hea, B., & MacKenzie, K. M. (2014). Trophic interactions of
636 fish communities at midwater depths enhance long-term carbon storage and benthic
637 production on continental slopes. *Proceedings of the Royal Society B: Biological Sciences*,
638 281(1787), 20140669. <https://doi.org/10.1098/rspb.2014.0669>
- 639 van Denderen, P. D., Lindegren, M., MacKenzie, B. R., Watson, R. A., & Andersen, K. H.
640 (2018). Global patterns in marine predatory fish. *Nature Ecology & Evolution*, 2(1), 65–70.
641 <https://doi.org/10.1038/s41559-017-0388-z>
- 642 Villéger, S., Brosse, S., Mouchet, M., Mouillot, D., & Vanni, M. J. (2017). Functional ecology of
643 fish: current approaches and future challenges. *Aquatic Sciences*, 79(4), 783–801.
644 <https://doi.org/10.1007/s00027-017-0546-z>
- 645 Watson, R. A., & Tidd, A. (2018). Mapping nearly a century and a half of global marine fishing:
646 1869–2015. *Marine Policy*, 93, 171–177. <https://doi.org/10.1016/j.marpol.2018.04.023>
- 647 Wei, C.-L., Rowe, G. T., Escobar-Briones, E., Boetius, A., Soltwedel, T., Caley, M. J., Soliman,
648 Y., Huettmann, F., Qu, F., Yu, Z., Pitcher, C. R., Haedrich, R. L., Wicksten, M. K., Rex, M.
649 A., Baguley, J. G., Sharma, J., Danovaro, R., MacDonald, I. R., Nunnally, C. C., ...
650 Narayanaswamy, B. E. (2011). Global patterns and predictions of seafloor biomass using
651 random forests. *PLOS ONE*, 5(12), e15323. <https://doi.org/10.1371/journal.pone.0015323>
- 652 Wilson, R. W., Millero, F. J., Taylor, J. R., Walsh, P. J., Christensen, V., Jennings, S., & Grosell,
653 M. (2009). Contribution of fish to the marine inorganic carbon cycle. *Science*, 323(5912),
654 359–362. <https://doi.org/10.1126/science.1157972>

655 **Figures captions**

656 Figure 1. Illustration of simplified fish guilds in the fish community deemed important for
657 global fisheries catches and active carbon export to depth. Fish interact with each other and the
658 resources through predator-prey interactions if they overlap in their spatial distribution in the
659 water column and if the prey is of preferred size (see inset).

660 Fig 2. Vertical position (blue lines) of fish guild size-classes and resources from a seafloor depth
661 of 100 to 3000 meters, described by the upper edge of the sloping yellow shape in each panel.
662 The vertical position shows the depth of maximum concentration z_c for day and night; two lines
663 indicate a bimodal vertical distribution (SI 1, Table S1.3). The euphotic depth is here set at 150
664 m. Note that there are more fish size-classes (SI 2) than the groups presented here, but the classes
665 align with the weight boundaries in each panel.

666 Figure 3. Emergent food web types from shelf regions to open ocean environments due to
667 seafloor depth, zooplankton production and detrital export reaching the seafloor. The food web
668 panels (a-e) show biomass in g wet weight per m^{-2} (circles; see reference biomass in lower right
669 corner) and fluxes of biomass in $g\ wet\ weight\ m^{-2}\ y^{-1}$ (lines) in a 1° grid cell. Dashed, solid thin
670 and solid thick lines show weak (0.01-0.1), intermediate (0.1-1) and strong (>1) feeding
671 interactions. Interactions less than $0.01\ g\ wet\ weight\ m^{-2}\ y^{-1}$ are not shown. The vertical position
672 of fish in the food web panels is the average position of each size class. The colors in the food
673 web panels correspond to the legend. The colors in the map (f) define regions with a similar food
674 web type, corresponding to the color in the panel title bars; threshold values are presented in SI 1
675 Table S1.4. Food web panels are not presented for the white regions where the resource
676 production is too low to support fish biomass.

677 Figure 4. Comparison of biomass and energy flow between the trait-based fish model (right) and
678 three regional-specific Ecopath with Ecosim (EwE) food web models (left). All panels show
679 biomass (circles, with values in $g\ wet\ weight\ m^{-2}$) and fluxes of biomass (lines, with values in g
680 $wet\ weight\ m^{-2}\ y^{-1}$). The circles and lines are both scaled with a \log_{10} transformation for
681 visualization. The internal loops present feeding fluxes within each grouping. No values are
682 included for lines with a flux $< 0.5\ g\ wet\ weight\ m^{-2}\ y^{-1}$.

683 Figure 5. Map of two fish ecosystem functions: potential fisheries production (a) and benthic-
684 pelagic coupling by demersal fish (b). Potential fisheries production is estimated as a fraction of

685 energy flowing from juveniles to the fished adults. Benthic-pelagic coupling by demersal fish is
686 estimated as the sum of all feeding fluxes from pelagic prey to demersal fish relative to the total
687 flux. This prediction does not consider cannibalism by demersal fish and is only shown in areas
688 where demersal biomass is $> 10^{-4}$ g wet weight m^{-2} .

689 Figure 6. Biomass of fish guilds as a function of seafloor depth for high (a), intermediate (b) and
690 low (c) zooplankton production and detrital export flux out of the euphotic zone. Benthic
691 maximum production depends on the detrital export flux and bottom depth, following eq. S21 in
692 SI 1 Table S1.1. The euphotic depth is at 150 m. Note the different scales on the y-axes.
693 Resource values: maximum small and large zooplankton production is 100 (a), 50 (b) and 5 (c) g
694 wet weight $m^{-2} y^{-1}$; detrital export flux is 380 (a), 250 (b) and 130 (c) g wet weight $m^{-2} y^{-1}$. There
695 is no variation in temperature (see SI 1 Fig S1.3 for results for three different water column
696 temperatures).

697

698 **Supplementary material information**

699 Supplement 1: Supplementary tables and figures

700 Supplement 2: Fish community model formulation

701 Supplement 3: Input parameters for the global predictions on a 1° grid

702 Supplement 4: Resource productivity and water column temperature scenarios

703 Supplement 5: Discretization of fish size-classes

704 Supplement 6: Model comparison with Ecopath with Ecosim